Functional in vitro characterization of SLCO1B1 variants and simulation of the clinical pharmacokinetic impact of impaired OATP1B1 function

Kiander, Wilma

2022-09-01

Kiander , W , Sjostedt , N , Manninen , R , Jaakkonen , L , Vellonen , K-S , Neuvonen , M , Niemi , M , Auriola , S & Kidron , H 2022 , ' Functional in vitro characterization of SLCO1B1 variants and simulation of the clinical pharmacokinetic impact of impaired OATP1B1 function ' , European Journal of Pharmaceutical Sciences , vol. 176 , 106246 . https://doi.org/10.1016/j.ejps.2022.106246

http://hdl.handle.net/10138/346696
https://doi.org/10.1016/j.ejps.2022.106246

European Journal of Pharmaceutical Sciences 176 (2022) 106246

Contents lists available at ScienceDirect

European Journal of Pharmaceutical Sciences

journal homepage: www.elsevier.com/locate/ejps

Functional *in vitro* characterization of *SLCO1B1* variants and simulation of the clinical pharmacokinetic impact of impaired OATP1B1 function.

Wilma Kiander [a], Noora Sjöstedt [a], Riikka Manninen [a], Liina Jaakkonen [a], Kati-Sisko Vellonen [b], Mikko Neuvonen [c,d], Mikko Niemi [c,d,e], Seppo Auriola [b], Heidi Kidron [a,*]

[a] Division of Pharmaceutical Biosciences, Faculty of Pharmacy, University of Helsinki, Helsinki, Finland
[b] School of Pharmacy, University of Eastern Finland, Kuopio, Finland
[c] Department of Clinical Pharmacology, Faculty of Medicine, University of Helsinki, Helsinki, Finland
[d] Individualized Drug Therapy Research Program, Faculty of Medicine, University of Helsinki, Helsinki, Finland
[e] Department of Clinical Pharmacology, HUS Diagnostic Center, Helsinki University Hospital, Helsinki, Finland

ARTICLE INFO

Keywords:
Pharmacogenetics
Rosuvastatin
Pharmacokinetics
Simulation
Proteomics

ABSTRACT

Organic Anion Transporting Polypeptide 1B1 is important to the hepatic elimination and distribution of many drugs. If OATP1B1 function is decreased, it can increase plasma exposure of *e.g.* several statins leading to increased risk of muscle toxicity. First, we examined the impact of three naturally occurring rare variants and the frequent *SLCO1B1* c.388A>*G* variant on *in vitro* transport activity with cellular uptake assay using two substrates: 2′, 7′-dichlorofluorescein (DCF) and rosuvastatin. Secondly, LC–MS/MS based quantitative targeted absolute proteomics measured the OATP1B1 protein abundance in crude membrane fractions of HEK293 cells over-expressing these single nucleotide variants. Additionally, we simulated the effect of impaired OATP1B1 function on rosuvastatin pharmacokinetics to estimate the need for genotype-guided dosing. R57Q impaired DCF and rosuvastatin transport significantly yet did not change protein expression considerably, while N130D and N151S did not alter activity but increased protein expression. R253Q did not change protein expression but reduced DCF uptake and increased rosuvastatin K_m. Based on pharmacokinetic simulations, doses of 30 mg (with 50% OATP1B1 function) and 20 mg (with 0% OATP1B1 function) result in plasma exposure similar to 40 mg dose (with 100% OATP1B1 function). Therefore dose reductions might be considered to avoid increased plasma exposure caused by function-impairing OATP1B1 genetic variants, such as R57Q.

1. Introduction

Organic Anion Transporting Polypeptide 1B1 (OATP1B1) facilitates the hepatic uptake of a wide variety of endogenous compounds and drugs such as the lipid-lowering statins (Niemi et al., 2011). Statins are effective in the primary and secondary prevention of myocardial infarction and are widely used (Baigent et al., 2005). As OATP1B1 substrates, these drugs are susceptible to pharmacokinetic changes caused by altered OATP1B1 function. This can lead to treatment failures, adverse effects and discontinuation of statin treatment which may result in an increased incidence of cardiovascular events and mortality (De Vera et al., 2014).

Single nucleotide variants (SNVs) in the *SLCO1B1* gene that encodes OATP1B1 can impair the transporter function. For example, the *SLCO1B1* c.521T>C variant increases plasma concentrations of several statins and subsequently the risk for adverse reactions ranging dose-dependently from myalgia to rhabdomyolysis (Niemi et al., 2011). The European Society of Cardiology and the European Atherosclerosis Society have released new guidelines for the treatment of dyslipidemias with stricter low-density lipoprotein cholesterol (LDL-C) goals for high-risk patients (Mach et al., 2020). Higher doses of statins may be required to reach these target LDL-C levels, which, in turn, would increase the likelihood of adverse effects in patients carrying function-impairing genotypes of *SLCO1B1*. Genotyping can be utilized to avoid unsuitable dosing, providing knowledge on the possible impact of the genotype is available. This information, however, is lacking when it comes to rare SNVs.

The three-dimensional structure of OATP1B1 remains unsolved and the underlying mechanisms for substrate binding and/or recognition are largely unknown. Many critical amino acids in the putative

* Corresponding author.
E-mail address: heidi.kidron@helsinki.fi (H. Kidron).

https://doi.org/10.1016/j.ejps.2022.106246
Received 18 February 2022; Received in revised form 9 June 2022; Accepted 20 June 2022
Available online 22 June 2022

transmembrane region have been identified in previous *in vitro* studies (Hong, 2014; Kiander et al., 2021). Less is known about the importance of amino acids in the extracellular loops (ECLs) of OATP1B1. ECLs host many sites for post-translational modifications that affect the proper function and localization of transporters (Lee et al., 2020). Yet, beyond these modifications, the significance of the amino acids in the ECLs remains largely unexplored.

The current study examines how *SLCO1B1* SNVs located in the predicted ECLs of OATP1B1 (Table 1, Fig. 1, Supplementary Table III) affect the transport activity and membrane abundance *in vitro* to improve the understanding of the significance of ECLs in OATP1B1 expression and function. Furthermore, we estimate the clinical effect of impaired OATP1B1 function on clinical rosuvastatin pharmacokinetics with a pharmacokinetic simulation model. Combining these simulations with *in vitro* activity data could allow the identification of SNVs that could warrant caution when prescribing rosuvastatin.

2. Materials and methods

2.1. Materials

Q5® Site-Directed Mutagenesis Kit was purchased from New England Biolabs (Ipswich, MA, USA) and Oligomer (Helsinki, Finland) produced the mutagenesis primers. Fetal bovine serum (FBS), Hank's Balanced Salt Solution (HBSS), Dulbecco's Modified Eagle Medium (DMEM), Coomassie Plus protein assay reagent and HyClone SfX Insect cell medium were from ThermoFisher Scientific (Waltham, MA, USA). 2′,7′-dichlorofluorescein (DCF) was from Santa Cruz Biotechnology (Dallas, TX, USA) and rosuvastatin hemicalcium and rosuvastatin-d6 sodium salt from Toronto Research Chemicals (North York, ON, Canada). ProteaseMax surfactant, Lys-C endopeptidase and tosylphenylalanylchloromethyl ketone (TPCK) -treated trypsin were from Promega (Madison, WI, USA). The peptide standards for Multiple Reaction Monitoring (MRM) analysis were from JPT Peptide Technologies GmbH (Berlin, Germany). All the other chemicals were purchased from Sigma-Aldrich (Saint Louis, MO, USA).

2.2. Preparation of plasmids carrying SLCO1B1 variant forms

The SNVs were selected based on their location in the ECLs and the changes (such as loss of charge) caused in the physical properties of the OATP1B1 secondary structure (Table 1, Fig. 1). The selected rare variants have a total minor allele frequency of less than 0.0004 (Supplementary Table III). The pENTR plasmids carrying the *SLCO1B1* gene and the gene for enhanced yellow fluorescent protein (eYFP, negative control) (El-Sheikh et al., 2007) were a kind gift from Jan Koenderink (Radboud Institute for Molecular Life Sciences, Nijmegen, the Netherlands). The single nucleotide variants were introduced into the reference *SLCO1B1* gene (Genebank™ accession number AJ132573.1) with the Q5® Site-Directed Mutagenesis Kit. Used primers are listed in Supplementary Table I. The correct sequence of the SNVs in pENTR221 entry vector was verified by GATC Biotech sequencing service (Constance, Germany) (data not shown).

Table 1
The *SLCO1B1* single nucleotide variants included in the study and predicted consequences of the amino acid changes.

SNV	Amino acid change	Variant ID	SIFT prediction[a]	PolyPhen prediction[b]
c.170G>*A*	Arg57Gln	rs61760182	deleterious	probably damaging
c.388A>*G*	Asn130Asp	rs2306283	tolerated	benign
c.452A>*G*	Asn151Ser	rs2306282	tolerated	benign
c.758G>*A*	Arg253Gln	rs11045853	deleterious	probably damaging

[a] SIFT Human Protein online service (11) (http://sift.jcvi.org/www/SIFT_enst_submit.html).
[b] the Poly-Phen 2 service (10) (http://genetics.bwh.harvard.edu/pph2/) using the human OATP1B1 protein sequence.

2.3. Cell culture and protein expression

Human Embryonic Kidney (HEK293) cells were used to over-express the OATP1B1 variants as they lack endogenous OATP proteins (Ahlin et al., 2009). The cells were cultured in DMEM, high-glucose, GlutaMax culture medium supplemented with 10% FBS at 37 °C, 5% CO_2. For the uptake assays, the cells (0.5 *10^6 per well) were seeded on Nunc™ 48-well plates coated with poly-d-lysine in-house (Thermo Fisher Scientific). Twenty-four hours later medium was changed and the cells were transduced with the baculoviruses, supplemented with expression-stimulating sodium butyrate (final concentration of 5 mM, in-house optimization, data not shown).

We produced the baculoviruses carrying the reference and mutated *SLCO1B1* genes and over-expressed the proteins following the previously published protocol (Kiander et al., 2021; Sjöstedt et al., 2017; Tikkanen et al., 2020). With the purpose of limiting the variability in the expression system, two separate batches of baculoviruses were produced with standardized amount of DNA in each batch and the variants were only compared to the batch specific reference OATP1B1 virus. While virus titer or multiplicity of infection (MOI) was not determined, the infection parameters were optimized empirically with titration experiments to obtain the level of maximum transduction and this ratio was then used in all experiments.

2.4. Cellular uptake assays

The cellular uptake assay ensued 48 h post-transduction on a heated (37 °C) orbital shaker plate. The medium was replaced with 500 μl of transport buffer (HBSS with 4.2 mM $NaHCO_3$ and 25 mM HEPES adjusted to pH 7.4 with NaOH) and preincubated for 3 min. Following the removal of the buffer, the uptake was initiated with the addition of 125 μl of test solution containing the test compound (rosuvastatin or DCF) in transport buffer. The uptake was terminated within the linear uptake phase with the aspiration of the test solution: at 2 min for rosuvastatin and at 15 min for DCF, followed by a three-time wash with 500 μl of ice-cold transport buffer. The cells were lysed with 125 μl of appropriate lysis buffer (3:1 methanol-water mixture containing 25 ng/ml rosuvastatin-D6 as an internal standard for rosuvastatin and 0.1 M NaOH for DCF samples). Rosuvastatin samples were centrifuged (14,000 g, 10 min) and rosuvastatin in the supernatant was quantified as described below. DCF in the cell lysate was analyzed with fluorescence measurement (excitation 500 nm, emission 528 nm, bandwidth 5 nm) using the multimode microplate reader Varioskan LUX (Thermo Fisher Scientific, Vantaa, Finland). For total protein quantification, 10 μl of cell lysate was mixed with 300 μl Coomassie Plus reagent followed by absorbance analysis (595 nm) with Varioskan LUX.

2.5. Rosuvastatin LC-MS/MS analysis

Rosuvastatin concentrations in the methanol-water supernatant samples were analyzed with a previously published method (Deng et al., 2021) using a Sciex 5500Qtrap LC/MSMS system (ABSciex) interfaced with an electrospray ionization (ESI) source. The chromatographic separation was achieved on a Luna Omega polar C18 column (100 × 2.1 mm I.D., 1.6 μm particle size; Phenomenex, Torrance, CA, USA) using 5 mM ammonium formate (pH 3.9, adjusted with 98% formic acid) as mobile phase A and acetonitrile as mobile phase B. The mobile phase gradient program was as follows: 1 min at 20% B on hold, then a linear ramp from 20% B to 40% B over 3 min followed by a second linear ramp to 90% B over 2 min, and 1 min at 90% B before a re-equilibration step back to the initial conditions (20% B). The flow rate and the column temperature were maintained at 300 μL/min and 40 °C. Rosuvastatin

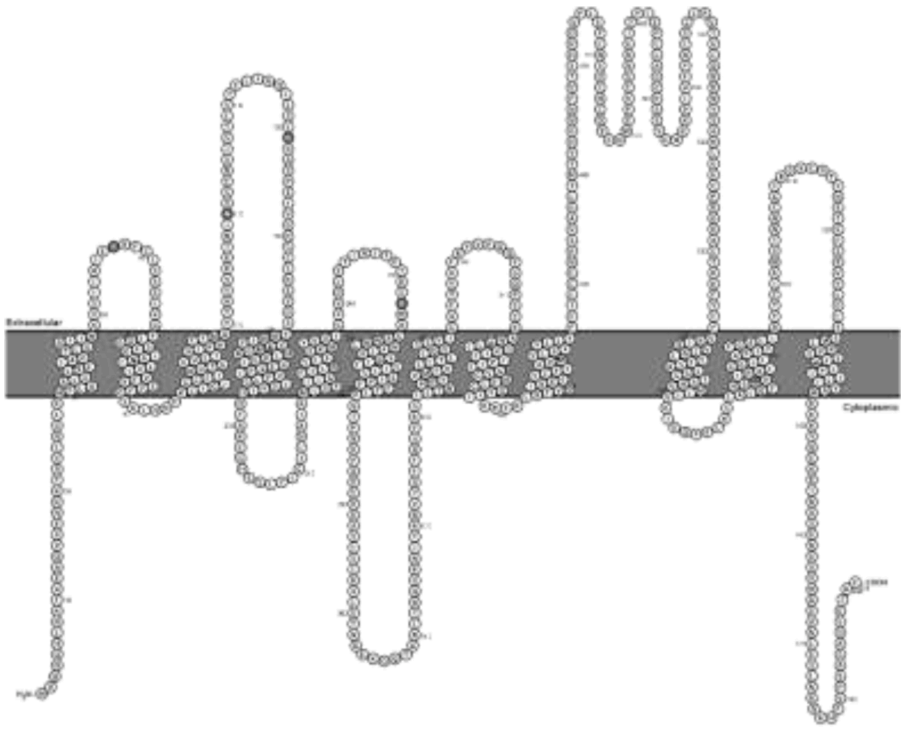

Fig. 1. Location of the amino acids affected by the selected single nucleotide variants in the predicted extracellular loops of OATP1B1. The figure is based on the Uniprot entry Q9Y6L6 and generated with Protter (Omasits et al., 2014).

and the internal standard, rosuvastatin-D6, were detected in positive multiple reaction monitoring mode using the characteristic mass-to-charge (*m/z*) ion transitions 482–258 and 488–264. The lower limit of quantification (LLOQ) for rosuvastatin was 0.1 ng/mL. The between-run precision was below 15% (expressed as CV%) and the between-run accuracy was within ±15%, except for LLOQ, for which both precision and accuracy were within ±20%

2.6. Pharmacokinetic model and simulation

Pharmacokinetic simulations were performed using the SimBiology 6.0 application in MATLAB (version 2020b, Mathworks, Natick, MA, USA) with the ode15s/NDF solver. The model is based on a published minimal physiologically-based pharmacokinetic rosuvastatin model (Bosgra et al., 2014). The model consists of a stomach, intestine and a single central compartment (Supplementary Fig. 1). Hepatic disposition is described using a liver dispersion model with a series of four consecutive liver subcompartments, each with an extrahepatic and intracellular compartment (Supplementary Fig. 1). Enterohepatic circulation is also included in the model. The parameters used in the model were the same as described previously (Bosgra et al., 2014), except for the contribution of OATP1B1 to the total intrinsic influx clearance of rosuvastatin. This was set to 51% of the total intrinsic influx clearance (or 532 L/h) based on the average calculated from different studies predicting the individual contribution of OATP1B1 to rosuvastatin uptake in the liver (Bosgra et al., 2014; Kitamura et al., 2008; Kunze et al., 2014; Zhang et al., 2019). The structure of the model was validated by reproducing the simulations in the original Bosgra et al. (2014) publication and by comparing simulations to genotyped *SLCO1B1*×*1/*1* (the reference genotype) clinical data (Birmingham et al., 2015; Pasanen et al., 2007; Wu et al., 2017). OATP1B1 function was set to 0 in the *SLCO1B1* c.521CC genotype simulations, based on our previous *in vitro* characterization, where the *SLCO1B1* c.521T>C SNP rendered OATP1B1 completely non-functional (Kiander et al., 2021). The effect of renal impairment on rosuvastatin renal clearance was estimated based on changes reported in the literature (Tatosian et al., 2021; Tzeng et al., 2008). Normal renal clearance of rosuvastatin was set to 13.9 L/h, while CL_R in moderate renal impairment was 6.8 L/h.

2.7. Crude membrane extraction

Crude membrane fractions were prepared from reference or variant OATP1B1 expressing HEK293 cells as described in Kiander et al. (2021). Cells cultured in T175 flasks were collected, centrifuged (3000 g, 15 min) and broken down with a Dounce tissue homogenizer. The supernatant resulting from 30-min centrifugation (3220 g, 4 °C) was separated and centrifuged again (21,000 g, 4 °C, 99 min). The formed pellet was resuspended in TS buffer (10 mM Tris-HEPES, 250 mM sucrose, pH 7.4) and protein content quantified as described previously.

2.8. LC-MS/MS based quantitative targeted absolute proteomics (QTAP) analysis

LC-MS/MS-based QTAP approach was applied to the quantification of the absolute protein expression of OATP1B1 in the crude membrane preparations as described previously (Kiander et al., 2021). After denaturation and break-down of the tertiary structure of the proteins, 50 μg of crude membrane preparations were digested first with 1/100 LysC endopeptidase and after that with 1/100 TPCK-treated trypsin. The previously used 150 pmol of isotope-labeled peptide mixture served as internal standard (Kiander et al., 2021).

Quantification was conducted with 6495 QQQ MS with 1290 HPLC system and AdvanceBio peptide Map Column, 2.7 μm, 2.1 × 250 mm (Agilent Technologies, Santa Clara, CA, USA) as described previously (Huttunen et al., 2019). MS conditions were: 30 μl injection volume, ESI positive ion mode, source temperature 210 °C, drying gas (nitrogen) flow rate 15 L/min, nebulizer pressure 45 psi, MS capillary voltage 3 kV and dwell time 40 ms. The SNVs did not alter the amino acids in the analyzed peptide sequences (Kiander et al., 2021). The peak area ratios of the analyte peptides and their respective internal standards were compared with Skyline application (MacCoss Lab Software, Seattle, WA). The results of OATP1B1 expression are presented as relative to the

Na^+/K^+-ATPase expression level and normalized to the reference OATP1B1 protein.

2.9. Data analysis

The uptake of test substrates was normalized to total protein amount in the well. OATP1B1-mediated transport was calculated by subtracting the uptake into eYFP expressing cells (representing passive influx) from uptake into OATP1B1-expressing cells. The OATP1B1-mediated transport into variant cells was then normalized to the reference OATP1B1 cells.

Cellular uptake assays were conducted in triplicate in three to five separate experiments and the average of the technical triplicates is considered as one data point. The proteomics samples were prepared from three batches of HEK293 cells. The data are presented as their mean ± SEM.

The statistical significance of the differences in activity and expression levels of the variants compared to the reference was determined with Kruskal–Wallis one-way analysis of variance with Dunn's post hoc test for multiple comparisons (GraphPad Prism 6.05, GraphPad Software, San Diego, CA, USA). Tukey's multiple comparisons test assessed whether the uptake of of DCF and rosuvastatin differed from each other to a statistically significant degree.

Maximum velocity (V_{max}) and Michaelis-Menten constant (K_m) values of rosuvastatin transport were calculated with non-linear regression from concentration-dependent cellular uptake data and uptake values were normalized to reference OATP1B1 V_{max}. The extra-sum-of-squares F-test was used to assess the statistical significance of differences in K_m and V_{max} values between the reference and the variants. P-values below 0.05 were considered significant in all analyses.

3. Results

Four naturally occurring SNVs located in the ECLs of OATP1B1 were expressed in HEK293 cells and their effect on transport function was assessed using two substrates (Figs. 2 and 3). LC-MS/MS-based QTAP approach quantified any changes in protein abundance of OATP1B1 in crude membrane fractions (Fig. 4).

R57Q impaired the uptake of DCF significantly ($P < 0.05$) compared to the reference (Fig. 2). A noticeable reduction in activity was also observed in R253Q: the transport was less than 50% of the reference. N130D and N151S, on the other hand, did not alter transport activity.

N130D, N151S and R253Q did not change the maximum velocity (V_{max}) of OATP1B1-mediated rosuvastatin transport significantly (Table 2). However, R57Q caused a significant ($P < 0.05$) impairment in rosuvastatin transport comparable to the reduction observed in DCF transport (Table 2, Figs. 2 and 4). R57Q V_{max} was on average only 11% of the reference. Nevertheless, R57Q, along with N130D and N151S, did not alter apparent affinity (K_m) of rosuvastatin to OATP1B1 (Table 2). In contrast, R253Q decreased the affinity of OATP1B1 to rosuvastatin, leading to an average K_m value of 31 μM compared to 13 μM of wild-type OATP1B1 (Table 2). No significant substrate dependent differences between 1 μM DCF and 5 μM rosuvastatin were observed.

While no statistically significant alterations in OATP1B1 protein expression in the crude membrane fractions were observed, N130D and N151S variants interestingly increased the protein expression of OATP1B1 and R57Q decreased the protein expression (Fig. 4, Table 2).

The effect of OATP1B1 variants on rosuvastatin pharmacokinetics was evaluated with a physiologically-based pharmacokinetic model (Supplementary Fig. 1). The model imitated previous simulations of Bosgra et al. (2014) and was able to capture plasma concentrations of rosuvastatin in *SLCO1B1*1/*1* subjects (the reference genotype) (Supplementary Fig. 2 A-C). The simulated C_{max} and AUC were within 2-fold of the observed parameters, which is generally regarded as acceptable (Supplementary Table IV). The time to maximum concentration, however, was somewhat underestimated but within the range of observed values (Fig. 5A, Supplementary Fig. 2 B and C, Supplementary Table IV). Simulations with multiple dosing resulted in only slight, clinically insignificant accumulation (Supplementary Fig. 2 D), thus subsequent simulations were performed as single-dose scenarios.

Next, the effect of *SLCO1B1* c.521T>C genotype was simulated based on a clinical study (Pasanen et al., 2007). In the clinical study, homozygotes for *SLCO1B1* c.521T>C had approximately 65% higher rosuvastatin AUC and 79% higher C_{max} values compared to carriers of the reference genotype. The simulation over-predicted the AUC and C_{max} of both genotypes, but the simulated proportional increase in AUC and C_{max} with the c.521CC genotype was comparable with the clinical observations (Fig. 5A). The AUC and C_{max} of rosuvastatin increased

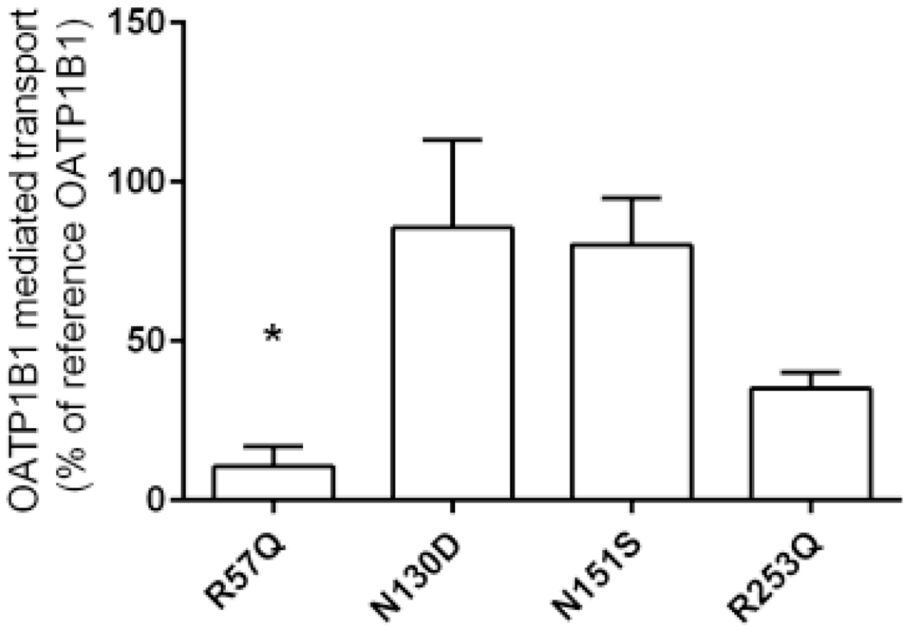

Fig. 2. OATP1B1 mediated transport of 1 μM DCF into HEK293 cells over 15 min. Results are calculated as mean of five experiments conducted in triplicates and represented as % of reference OATP1B1 transport ± SEM ($n = 5$). * = $P < 0.05$ (compared to the reference.).

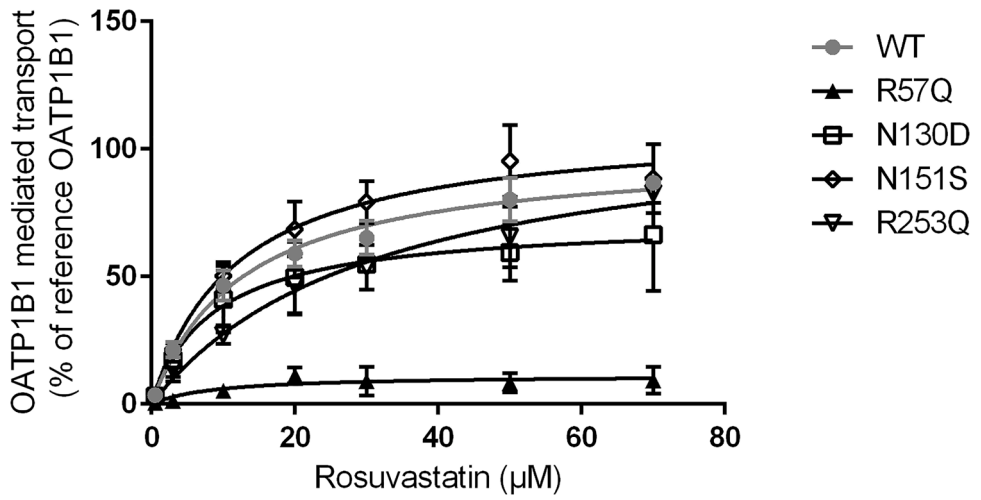

Fig. 3. Kinetics of OATP1B1-mediated rosuvastatin transport into HEK293 cells for 2 min. Results are calculated as mean of three experiments conducted in triplicates and represented as % of reference OATP1B1 transport ± SEM ($n = 3$).

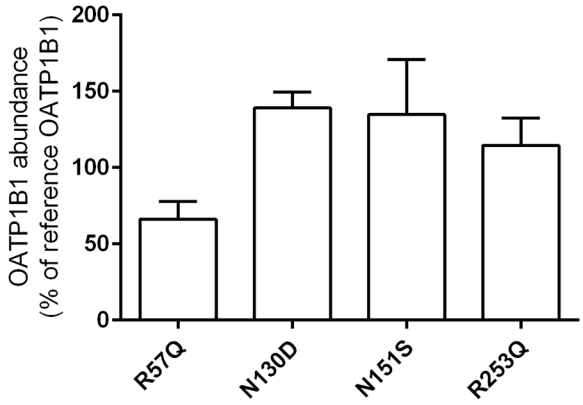

Fig. 4. LC-MS/MS proteomic analysis of 50 μg HEK293 crude membrane preparations expressing variant OATP1B1. Abundance of OATP1B1 was quantified in three independent samples, normalized to Na^+/K^+-ATPase and reference OATP1B1 abundance (100%). The results are presented as mean ± SEM ($n = 3$).

linearly when the activity of OATP1B1 decreased and total loss-of-function of OATP1B1 was predicted to lead to a 79% increase in rosuvastatin AUC and an 89% increase in C_{max} (Fig. 5B, Table 3). Time to maximum plasma concentration (T_{max}) remained unaffected.

When OATP1B1 activity was set to 50% of the reference genotype in simulations, a 30 mg single dose resulted in AUC and C_{max} values similar to a 40 mg dose with fully functional OATP1B1 (Fig. 5C, Table 3). If OATP1B1 was entirely non-functional, only a 20 mg dose was required to achieve the same plasma exposure. The liver exposure, however, declined along with the dosing changes and the liver AUC of 20 mg dose in the non-functional OATP1B1 scenario was 44% of the liver exposure of 40 mg dose in the fully functional OATP1B1 scenario (Table 3).

The 40 mg dose is contraindicated in patients with pre-disposing factors for myopathy/rhabdomyolysis such as moderate renal impairment (Crestor Summary of Product Characteristics European Medicines Agency (EMA), 2005). Since *SLCO1B1* polymorphism is also a pre-disposing factor and the next available dosage form is a 20 mg tablet, the possible additive effect of renal impairment to rosuvastatin pharmacokinetics of 20 mg dose was simulated in moderate renal impairment with or without OATP1B1 impairment. The plasma exposure in the scenario with 20 mg single dose in moderate renal impairment and normal OATP1B1 function was comparable to the exposure resulting from 10 mg dose in individuals with moderate renal impairment and no OATP1B1 function (Fig. 5D). In opposition to the changes in plasma exposure, the liver exposure decreased linearly with dose (Fig. 5C and D).

4. Discussion

Cholesterol-lowering statins, such as rosuvastatin, are an established part of the primary and secondary prevention of coronary heart disease, stroke and peripheral artery disease (Kazi et al., 2017). As an OATP1B1 substrate, rosuvastatin is susceptible to the pharmacokinetic changes SNVs in the *SLCO1B1* gene can cause but knowledge on the effect of rare SNVs on rosuvastatin transport is lacking. In this study, the transport activity and protein abundance of three rare *SLCO1B1* SNVs, R57Q, N151S and R253, along with the more frequent SNV N130D located in OATP1B1 extracellular loops were assessed *in vitro* (Figs. 2–4). The clinical pharmacokinetic effect of impaired OATP1B1 function was estimated with a pharmacokinetic model to assess suitable rosuvastatin doses for individuals harboring function-impairing genotypes of *SLCO1B1* (Fig. 5, Table 3).

R57Q is located in ECL1 of OATP1B1. A positive charge in a corresponding position is found in all human OATPs (Weaver and Hagenbuch, 2010), but this SNV changes the positively charged arginine into

Table 2
Compilation of results. Uptake and abundance data are normalized to the reference. Maximum velocity of transport (V_{max}) of the tested variants is normalized to the calculated V_{max} of reference OATP1B1. * = $P < 0.05$. Ref = reference (n values can be found in corresponding figures 2-4).

Variant	1 μM DCF uptake (% ref) ± SEM	5 μM Rosuvastatin uptake (% ref) ± SEM	Rosuvastatin K_m (μM) (95% CI)	Rosuvastatin V_{max} (% ref) (95% CI)	OATP1B1 abundance (% ref) ± SEM
Reference			12.5 (6.7 to 18.3)	100 (85.1 to 113.1)	
R57Q	10.6 ± 6.4	20 ± 9.3	8.9 (0 to 30.2)	11.4 (3.9 to 18.9)*	66 ± 11.6
N130D	85.6 ± 27.7	82 ± 33.6	8.7 (0 to 20.7)	72.2 (46.3 to 98.1)	139 ± 10.4
N151S	80.2 ± 14.7	101 ± 1.5	11.7 (3.3 to 20.2)	109.8 (86.4 to 133.1)	135 ± 36.1
R253Q	35 ± 5	62 ± 15.1	31.5 (5.4 to 57.6)*	114.4 (72 to 156.8)	115 ± 18

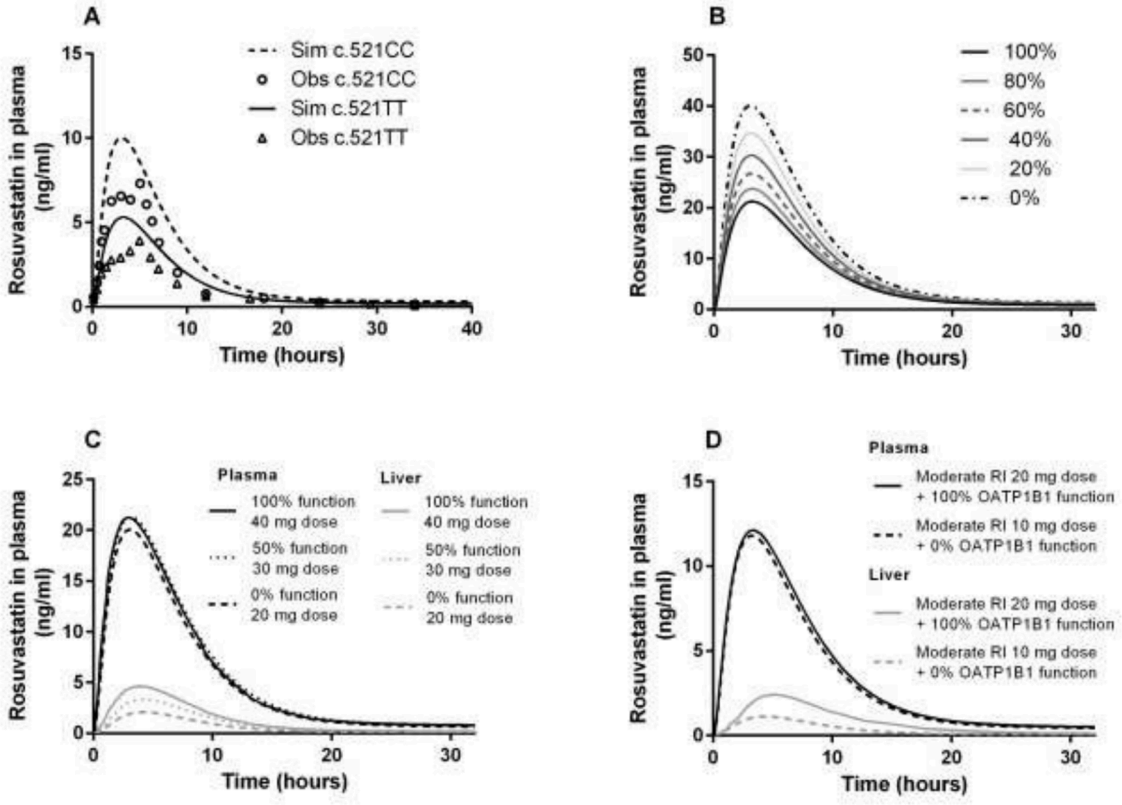

Fig. 5. Pharmacokinetic simulations of rosuvastatin. A: observed plasma concentrations in individuals homozygous for SLCO1B1 c.521T>C (open circles) and reference genotype (open triangles) (Pasanen et al., 2007) *vs.* simulated plasma concentrations after 10 mg single oral dose. B: the simulated effect of different degrees of OATP1B1 function after a 40 mg single oral dose. C: simulated plasma (black) and hepatic (gray) concentrations of rosuvastatin after different single doses and OATP1B1 activities. D: the simulated effect of dose reduction in subjects with moderate renal impairment (RI) and loss-of-function OATP1B1 genotype (dashed lines) on plasma (black) and hepatic (gray) concentrations of rosuvastatin.

polar, non-charged glutamine. In our study, this resulted in significantly decreased uptake of both DCF and rosuvastatin (Figs. 2 and 3). This effect does not appear to be substrate specific, since R57Q was previously shown to also reduce estrone-3-sulfate and cerivastatin transport significantly (Tamraz et al., 2013). The reduction in transport activity is not entirely explained by changes in protein abundance, which was reduced only by 34% (Fig. 4). A similar 30% reduction in protein abundance was previously observed in OATP1B1 HEK293 samples when this arginine at position 57 was replaced with aliphatic alanine in a site-directed mutagenesis study (Weaver and Hagenbuch, 2010). The R57A mutation also affected the apparent affinities toward different substrates. Interestingly, replacing R57 with a likewise charged lysine resulted in transport activity comparable to the reference and 20% increase in cell-surface expression. R57W, another rare SNV resulting in a loss-of-charge at this position, has been associated with reduced methotrexate clearance (Ramsey et al., 2012). Altogether, a positively charged amino acid at position 57 appears to be important for substrate translocation.

Two of the studied variants, N130D and N151S, are in ECL2. No prior *in vitro* data is available on the effects of amino acid changes in the position 151 on OATP1B1 function. In this study, N151S was shown to be benign: it did not alter the transport activity of either of the tested substrates and the protein abundance was similar to the reference OATP1B1 (Table 2). This is in accordance with the unaltered pravastatin pharmacokinetics observed in heterozygous carriers of N151S (Nishizato et al., 2003). Although no substrate-dependent differences were seen here, in previous *in vitro* studies, N130D has shown unaltered, reduced or enhanced transport depending on the substrate used to study activity (Ho et al., 2006; Lee et al., 2015; Michalski et al., 2002; Ramsey et al., 2012; Tirona et al., 2003, 2001). In our study the maximum velocity of rosuvastatin transport was slightly decreased but uptake of DCF and rosuvastatin was on average comparable to the reference (Figs. 2 and 3, Table 2). Clinically N130D (*SLCO1B1*37*) is considered a normal-function SNV (Cooper-DeHoff et al., 2022). N130D increases the protein expression of OATP1B1 which could lead to more active uptake, increasing non-renal clearance and lowering plasma exposure. This increased expression of OATP1B1 (up to 1.8-fold higher for homozygote N130D compared to the reference genotype) was previously observed in liver samples (Nies et al., 2013; Peng et al., 2015; Prasad et al., 2014). Our results from the QTAP analysis corroborate this: we observed ~1.4-fold higher OATP1B1 abundance in the N130D expressing HEK293 cells compared to the reference (Table 2).

R253Q is part of the highly conserved signature sequence of OATPs located in the boundary of ECL3 and transmembrane helix 6 (Taylor-Wells and Meredith, 2014), yet its role in OATP1B1 function remains unexplored. In this study, R253Q decreased the apparent affinity of rosuvastatin to OATP1B1 and reduced the uptake of DCF while the protein expression remained comparable to the reference OATP1B1 (Fig. 3, Table 2). These data suggest that R253Q affects the substrate recognition of OATP1B1 rather than the protein expression.

Pharmacokinetic simulations were carried out to estimate the clinical effect variants could have on rosuvastatin exposure. The contribution of OATP1B1 to total active uptake clearance has been estimated to be between 23 and 79% in *in vitro* studies (Bosgra et al., 2014; Kitamura et al., 2008; Kunze et al., 2014; Zhang et al., 2019). In our simulations, OATP1B1 contribution was set to the mean of these published values (51%). With this contribution, the observed increase in rosuvastatin AUC and C_{max} in subjects with the loss-of-function c.521CC genotype was adequately recovered with the simulation (Fig. 5A, Table 3). A moderate over-prediction was evident in comparison of the clinically

Table 3
Simulated pharmacokinetic parameters.

Scenario	Dose	$AUC_{0-48\ h}$ (ng*h/ml)	C_{max} (ng/ml(	Liver $AUC_{0-48\ h}$ (ng*h/ml)
Observed[a]				
c.521TT genotype	10 mg	34 ± 17.5	4.2 ± 2.4	N/A
c.521CC genotype	10 mg	56 ± 5.4	7.5 ± 1.2	N/A
Simulated				
c.521TT genotype	10 mg	51	5.3	11.6
c.521CC genotype[b]	10 mg	92	10	10.4
100% OATP1B1	40 mg	206	21.2	47
80% OATP1B1	40 mg	228	23.7	46.3
60% OATP1B1	40 mg	254	26.7	45.4
40% OATP1B1	40 mg	285	30.3	44.3
20% OATP1B1	40 mg	322	34.7	43
0% OATP1B1	40 mg	367	40	41.4
50% OATP1B1	30 mg	202	21.3	33.6
0% OATP1B1	20 mg	183	20	20.7
Moderate RI + 100% OATP1B1	20 mg	121	12.1	25
ModerateRI + 0% OATP1B1	10 mg	113	11.8	11.6

AUC = Area Under the concentration-time Curve (extent of exposure), C_{max} = maximum concentration, N/A = not available, RI = renal impairment. [a] (Pasanen et al., 2007. [b] OATP1B1 function set to 0%.

observed and simulated AUC and C_{max} values of c.521TT and c.521CC subjects (Fig. 5A). This is expected, since rosuvastatin has high inter-individual variability. However, the simulations were able to recover the relative change caused by the c.521CC genotype and therefore increased our confidence in our estimate of OATP1B1 contribution, the model and subsequent dosing suggestions. In a previous simulation study incorporating pharmacodynamics (PD) to pharmacokinetics, the PD response of c.521T>C SNV did not change significantly compared to the reference genotype and liver exposure of rosuvastatin was reduced by only 9.6% (Rose et al., 2014). Our simulations with 10 mg dose in c.521TT and c.521CC genotypes resulted in a similar 10.3% reduction in liver AUC (Table 3).

The maximum approved dose of rosuvastatin is 40 mg per day (Crestor Summary of Product Characteristics European Medicines Agency, EMA, 2005). In our simulations, when OATP1B1 function was 50% of normal, 30 mg of rosuvastatin resulted in similar AUC and C_{max} values to the 40 mg dose with normal OATP1B1 function (Fig. 5C, Table 3). If a total loss-of-function occurs, only 20 mg is needed to reach these values, hence individuals with function-impairing genotypes might be advised to limit the maximum dose of rosuvastatin to reduce the likelihood of adverse effects. This is in accordance with the Clinical Pharmacogenetics Implementation Consortium (CPIC) guideline that recommends limiting rosuvastatin dose to 20 mg in patients with poor function *SLCO1B1* phenotype (Cooper-DeHoff et al., 2022). Similarly, loss-of-function *SLCO1B1* genotype has an additive effect on rosuvastatin plasma exposure in moderate renal impairment (Fig. 5D) and limiting the dose to 10 mg would maintain similar plasma exposure as a 20 mg dose based on our simulations.

In addition to the more common *SLCO1B1* c.521T>C (present in function-impairing haplotypes **5* and **15*), the carriers of rare variants causing loss-of-function could benefit from genotype-guided rosuvastatin dosing. While there are few carriers of an individual rare SNV, globally the combined number of rare *SLCO1B1* SNV carriers can be significant and there may also be notable inter-ethnic variability within the presence of rare SNVs (Supplementary Table III). Rare pharmacogenetic variants are strongly enriched in mutations predicted to cause functional alterations (Ingelman-Sundberg et al., 2018) and thus it is more likely that rare variants would warrant caution in rosuvastatin treatment than common variants. Moreover, the increase in plasma concentrations might be even greater for other statins. For example, a 200–300% increase in simvastatin acid AUC has been observed in homozygous *SLCO1B1* c.521T>C carriers compared to the reference genotype and *SLCO1B1* c.170G>A was first identified in rhabdomyolysis cases (Mykkänen et al., 2022; Pasanen et al., 2006; Tamraz et al., 2013). While this model only estimated the effect of impaired OATP1B1 function on rosuvastatin, it is likely that the studied variants may alter pharmacokinetics of other OATP1B1 substrate drugs as well.

Based on the simulations, the suggested genotype-guided changes in rosuvastatin dosing would decrease the intrahepatic concentration and might subsequently alter the lipid-lowering effect (Fig. 5C and D, Table 3). However, rosuvastatin is a very potent HMG-CoA reductase inhibitor with IC_{50} of about 5 nM (Filppula et al., 2021) and rosuvastatin could reduce LDL-C by more than 40% already at a 10 mg dose (European Medicines Agency (EMA), 2005; Weng et al., 2010). Nonetheless, if patients with loss-of-function genotypes are unsuccessful in reaching their target LDL-C levels with the genotype-guided doses, combination therapy with another lipid-lowering drug might be safer than increasing rosuvastatin dose.

Based on our study, an over-expression system can be utilized to quantify the changes SNVs cause in protein expression and transport activity, thus providing data on rare SNVs for *in vitro-in vivo* extrapolation otherwise largely unattainable *in vivo*. The model in our study is based on clinical data on healthy volunteers of Caucasian descent and only covered one statin and two risk factors (pharmacogenetics of OATP1B1 and renal impairment). While plasma exposure is an important risk factor for statin-induced myopathy, more research is required to fully understand the interplay between pharmacogenetics and other factors such as drug-drug interactions, high age and hypothyroidism.

5. Conclusions

R57Q reduced DCF and rosuvastatin transport significantly while protein expression did not change significantly. N130D and N151S increased protein expression but did not alter activity, while R253Q reduced DCF uptake and increased rosuvastatin K_m with no change in protein expression. Therefore these amino acids appear to be more important for proper translocation or substrate recognition rather than protein expression. Based on the pharmacokinetic simulations, dose reductions could be utilized to avoid increased rosuvastatin plasma concentrations due to OATP1B1 genetic variation or renal impairment, while maintaining adequate hepatic concentrations for therapeutic effect.

Funding

We are grateful for the funding provided by Svenska Kulturfonden, Medicinska Understödsföreningen for Liv och Hälsa, DRA Consulting oy, Instrumentarium Science Foundation, Finnish Cultural Foundation, Sigrid Jusélius Foundation and the European Research Council (Grant Agreement 725,249). The UEF Metabolomics laboratory is supported by Biocenter Finland and Biocenter Kuopio.

CRediT authorship contribution statement

Wilma Kiander: Conceptualization, Formal analysis, Investigation, Methodology, Project administration, Validation, Visualization, Writing – original draft, Writing – review & editing. **Noora Sjöstedt:** Formal analysis, Investigation, Methodology, Validation, Visualization, Writing

– original draft, Writing – review & editing. **Riikka Manninen:** Methodology, Writing – review & editing. **Liina Jaakkonen:** Methodology, Writing – review & editing. **Kati-Sisko Vellonen:** Investigation, Writing – original draft, Writing – review & editing. **Mikko Neuvonen:** Investigation, Writing – original draft, Writing – review & editing. **Mikko Niemi:** Funding acquisition, Resources, Supervision, Writing – review & editing. **Seppo Auriola:** Methodology, Funding acquisition, Resources, Writing – review & editing. **Heidi Kidron:** Conceptualization, Formal analysis, Funding acquisition, Project administration, Validation, Resources, Supervision, Writing – original draft, Writing – review & editing.

Acknowledgments

We would like to thank Leena Pietilä, Olga Kaugonen, Alli Sinokki and Feng Deng for technical assistance as well as Dr. Yasuo Uchida for consultation on sample preparation of the proteomics samples. Dr. Mikko Gynther is acknowledged for the methodology in proteomics. We acknowledge the Drug Discovery and Chemical Biology Network for providing access to screening instrumentation.

Supplementary materials

Supplementary material associated with this article can be found, in the online version, at doi:10.1016/j.ejps.2022.106246.

References

Ahlin, G., Hilgendorf, C., Karlsson, J., Szigyarto, C.A.K., Uhlén, M., Artursson, P., 2009. Endogenous gene and protein expression of drug-transporting proteins in cell lines routinely used in drug discovery programs. Drug Metab. Dispos. Biol. Fate Chem. 37, 2275–2283. https://doi.org/10.1124/dmd.109.028654.

Baigent, C., Keech, A., Kearney, P.M., Blackwell, L., Buck, G., Pollicino, C., Kirby, A., Sourjina, T., Peto, R., Collins, R., Simes, R., Cholesterol Treatment Trialists' (CTT) Collaborators, 2005. Efficacy and safety of cholesterol-lowering treatment: prospective meta-analysis of data from 90,056 participants in 14 randomised trials of statins. Lancet Lond. Engl. 366, 1267–1278, 10.1016/S0140-6736(05)67394-1.

Birmingham, B.K., Bujac, S.R., Elsby, R., Azumaya, C.T., Wei, C., Chen, Y., Mosqueda-Garcia, R., Ambrose, H.J., 2015. Impact of ABCG2 and SLCO1B1 polymorphisms on pharmacokinetics of rosuvastatin, atorvastatin and simvastatin acid in Caucasian and Asian subjects: a class effect? Eur. J. Clin. Pharmacol. 71, 341–355. https://doi.org/10.1007/s00228-014-1801-z.

Bosgra, S., van de Steeg, E., Vlaming, M.L., Verhoeckx, K.C., Huisman, M.T., Verwei, M., Wortelboer, H.M., 2014. Predicting carrier-mediated hepatic disposition of rosuvastatin in man by scaling from individual transfected cell-lines *in vitro* using absolute transporter protein quantification and PBPK modeling. Eur. J. Pharm. Sci. Off. J. Eur. Fed. Pharm. Sci. 65, 156–166. https://doi.org/10.1016/j.ejps.2014.09.007.

Cooper-DeHoff, R.M., Niemi, M., Ramsey, L.B., Luzum, J.A., Tarkiainen, E.K., Straka, R. J., Gong, L., Tuteja, S., Wilke, R.A., Wadelius, M., Larson, E.A., Roden, D.M., Klein, T.E., Yee, S.W., Krauss, R.M., Turner, R.M., Palaniappan, L., Gaedigk, A., Giacomini, K.M., Caudle, K.E., Voora, D., 2022. The Clinical Pharmacogenetics Implementation Consortium (CPIC) guideline for SLCO1B1, ABCG2, and CYP2C9 and statin-associated musculoskeletal symptoms. Clin. Pharmacol. Ther. https://doi.org/10.1002/cpt.2557.

De Vera, M.A., Bhole, V., Burns, L.C., Lacaille, D., 2014. Impact of statin adherence on cardiovascular disease and mortality outcomes: a systematic review. Br. J. Clin. Pharmacol. 78, 684–698. https://doi.org/10.1111/bcp.12339.

Deng, F., Tuomi, S.-K., Neuvonen, M., Hirvensalo, P., Kulju, S., Wenzel, C., Oswald, S., Filppula, A.M., Niemi, M., 2021. Comparative hepatic and intestinal efflux transport of statins. Drug Metab. Dispos. 49, 750–759. https://doi.org/10.1124/dmd.121.000430.

El-Sheikh, A.A.K., van den Heuvel, J.J.M.W., Koenderink, J.B., Russel, F.G.M., 2007. Interaction of nonsteroidal anti-inflammatory drugs with multidrug resistance protein (MRP) 2/ABCC2- and MRP4/ABCC4-mediated methotrexate transport. J. Pharmacol. Exp. Ther. 320, 229–235. https://doi.org/10.1124/jpet.106.110379.

European Medicines Agency (EMA), 2005. Crestor Amended Summary of Product Characteristics https://www.ema.europa.eu/en/documents/referral/crestor-5-mg-article-29-referral-annex-i-ii-iii_en.pdf.

Filppula, A.M., Hirvensalo, P., Parviainen, H., Ivaska, V.E., Lönnberg, K.I., Deng, F., Viinamäki, J., Kurkela, M., Neuvonen, M., Niemi, M., 2021. Comparative hepatic and intestinal metabolism and pharmacodynamics of statins. Drug Metab. Dispos. https://doi.org/10.1124/dmd.121.000406.

Ho, R.H., Tirona, R.G., Leake, B.F., Glaeser, H., Lee, W., Lemke, C.J., Wang, Y., Kim, R.B., 2006. Drug and bile acid transporters in rosuvastatin hepatic uptake: function, expression, and pharmacogenetics. Gastroenterology 130, 1793–1806. https://doi.org/10.1053/j.gastro.2006.02.034.

Hong, M., 2014. Critical domains within the sequence of human organic anion transporting polypeptides. Curr. Drug Metab. 15, 265–270. https://doi.org/10.2174/1389200214666131229111118.

Huttunen, J., Gynther, M., Vellonen, K.-S., Huttunen, K.M., 2019. L-Type amino acid transporter 1 (LAT1)-utilizing prodrugs are carrier-selective despite having low affinity for organic anion transporting polypeptides (OATPs). Int. J. Pharm. 571, 118714 https://doi.org/10.1016/j.ijpharm.2019.118714.

Ingelman-Sundberg, M., Mkrtchian, S., Zhou, Y., Lauschke, V.M., 2018. Integrating rare genetic variants into pharmacogenetic drug response predictions. Hum. Genomics 12, 26. https://doi.org/10.1186/s40246-018-0157-3.

Kazi, D.S., Penko, J.M., Bibbins-Domingo, K., 2017. Statins for primary prevention of cardiovascular disease: review of evidence and recommendations for clinical practice. Med. Clin. N. Am. 101, 689–699. https://doi.org/10.1016/j.mcna.2017.03.001.

Kiander, W., Vellonen, K.S., Malinen, M.M., Gynther, M., Hagström, M., Bhattacharya, M., Auriola, S., Koenderink, J.B., Kidron, H., 2021. The Effect of Single Nucleotide Variations in the Transmembrane Domain of OATP1B1 on *in vitro* Functionality. Pharm. Res. https://doi.org/10.1007/s11095-021-03107-8.

Kitamura, S., Maeda, K., Wang, Y., Sugiyama, Y., 2008. Involvement of multiple transporters in the hepatobiliary transport of rosuvastatin. Drug Metab. Dispos. Biol. Fate Chem. 36, 2014–2023. https://doi.org/10.1124/dmd.108.021410.

Kunze, A., Huwyler, J., Camenisch, G., Poller, B., 2014. Prediction of organic anion-transporting polypeptide 1B1- and 1B3-mediated hepatic uptake of statins based on transporter protein expression and activity data. Drug Metab. Dispos. Biol. Fate Chem. 42, 1514–1521. https://doi.org/10.1124/dmd.114.058412.

Lee, H.H., Leake, B.F., Teft, W., Tirona, R.G., Kim, R.B., Ho, R.H., 2015. Contribution of hepatic organic anion-transporting polypeptides to docetaxel uptake and clearance. Mol. Cancer Ther. 14, 994–1003. https://doi.org/10.1158/1535-7163.MCT-14-0547.

Lee, W., Ha, J.M., Sugiyama, Y., 2020. Post-translational regulation of the major drug transporters in the families of organic anion transporters and organic anion-transporting polypeptides. J. Biol. Chem. 295, 17349–17364. https://doi.org/10.1074/jbc.REV120.009132.

Mach, F., Baigent, C., Catapano, A.L., Koskinas, K.C., Casula, M., Badimon, L., Chapman, M.J., De Backer, G.G., Delgado, V., Ference, B.A., Graham, I.M., Halliday, A., Landmesser, U., Mihaylova, B., Pedersen, T.R., Riccardi, G., Richter, D. J., Sabatine, M.S., Taskinen, M.-R., Tokgozoglu, L., Wiklund, O., ESC Scientific Document Group, 2020. 2019 ESC/EAS Guidelines for the management of dyslipidaemias: lipid modification to reduce cardiovascular risk: the Task Force for the management of dyslipidaemias of the European Society of Cardiology (ESC) and European Atherosclerosis Society (EAS). Eur. Heart J. 41, 111–188. https://doi.org/10.1093/eurheartj/ehz455.

Michalski, C., Cui, Y., Nies, A.T., Nuessler, A.K., Neuhaus, P., Zanger, U.M., Klein, K., Eichelbaum, M., Keppler, D., Konig, J., 2002. A naturally occurring mutation in the SLC21A6 gene causing impaired membrane localization of the hepatocyte uptake transporter. J. Biol. Chem. 277, 43058–43063. https://doi.org/10.1074/jbc.M207735200.

Mykkänen, A.J.H., Taskinen, S., Neuvonen, M., Paile-Hyvärinen, M., Tarkiainen, E.K., Lilius, T., Tapaninen, T., Backman, J.T., Tornio, A., Niemi, M., 2022. Genome-wide association study of simvastatin pharmacokinetics. Clin. Pharmacol. Ther. 35652242. https://doi.org/10.1002/cpt.2674 n/a. In press.

Niemi, M., Pasanen, M.K., Neuvonen, P.J., 2011. Organic anion transporting polypeptide 1B1: a genetically polymorphic transporter of major importance for hepatic drug uptake. Pharmacol. Rev. https://doi.org/10.1124/pr.110.002857.

Nies, A.T., Niemi, M., Burk, O., Winter, S., Zanger, U.M., Stieger, B., Schwab, M., Schaeffeler, E., 2013. Genetics is a major determinant of expression of the human hepatic uptake transporter OATP1B1, but not of OATP1B3 and OATP2B1. Genome Med. 5, 1. https://doi.org/10.1186/gm405.

Nishizato, Y., Ieiri, I., Suzuki, H., Kimura, M., Kawabata, K., Hirota, T., Takane, H., Irie, S., Kusuhara, H., Urasaki, Y., Urae, A., Higuchi, S., Otsubo, K., Sugiyama, Y., 2003. Polymorphisms of OATP-C (SLC21A6) and OAT3 (SLC22A8) genes: consequences for pravastatin pharmacokinetics. Clin. Pharmacol. Ther. 73, 554–565, 10.1016/S0009-9236(03)00060-2.

Omasits, U., Ahrens, C.H., Müller, S., Wollscheid, B., 2014. Protter: interactive protein feature visualization and integration with experimental proteomic data. Bioinformatics 30, 884–886. https://doi.org/10.1093/bioinformatics/btt607.

Pasanen, M.K., Fredrikson, H., Neuvonen, P.J., Niemi, M., 2007. Different effects of SLCO1B1 polymorphism on the pharmacokinetics of atorvastatin and rosuvastatin. Clin. Pharmacol. Ther. 82, 726–733. https://doi.org/10.1038/sj.clpt.6100220.

Pasanen, M.K., Neuvonen, M., Neuvonen, P.J., Niemi, M., 2006. SLCO1B1 polymorphism markedly affects the pharmacokinetics of simvastatin acid. Pharmacogenet. Genomics 16, 873–879. https://doi.org/10.1097/01.fpc.0000230416.82349.90.

Peng, K., Bacon, J., Zheng, M., Guo, Y., Wang, M.Z., 2015. Ethnic variability in the expression of hepatic drug transporters: absolute quantification by an optimized targeted quantitative proteomic approach. Drug Metab. Dispos. 43, 1045–1055. https://doi.org/10.1124/dmd.115.063362.

Prasad, B., Evers, R., Gupta, A., Hop, C.E.C.A., Salphati, L., Shukla, S., Ambudkar, S.V., Unadkat, J.D., 2014. Interindividual variability in hepatic organic anion-transporting polypeptides and P-glycoprotein (ABCB1) protein expression: quantification by liquid chromatography tandem mass spectroscopy and influence of genotype, age, and sex. Drug Metab. Dispos. Biol. Fate Chem. 42, 78–88. https://doi.org/10.1124/dmd.113.053819.

Ramsey, L.B., Bruun, G.H., Yang, W., Treviño, L.R., Vattathil, S., Scheet, P., Cheng, C., Rosner, G.L., Giacomini, K.M., Fan, Y., Sparreboom, A., Mikkelsen, T.S., Corydon, T. J., Pui, C.-H., Evans, W.E., Relling, M.V., 2012. Rare *versus* common variants in

pharmacogenetics: SLCO1B1 variation and methotrexate disposition. Genome Res. 22, 1–8. https://doi.org/10.1101/gr.129668.111.

Rose, R.H., Neuhoff, S., Abduljalil, K., Chetty, M., Rostami-Hodjegan, A., Jamei, M., 2014. Application of a physiologically based pharmacokinetic model to predict OATP1B1-related variability in pharmacodynamics of rosuvastatin. CPT Pharmacomet. Syst. Pharmacol. 3, e124. https://doi.org/10.1038/psp.2014.24.

Sjöstedt, N., van den Heuvel, J.J.M.W., Koenderink, J.B., Kidron, H., 2017. Transmembrane domain single-nucleotide polymorphisms impair expression and transport activity of ABC transporter ABCG2. Pharm. Res. 34, 1626–1636. https://doi.org/10.1007/s11095-017-2127-1.

Tamraz, B., Fukushima, H., Wolfe, A.R., Kaspera, R., Totah, R.A., Floyd, J.S., Ma, B., Chu, C., Marciante, K.D., Heckbert, S.R., Psaty, B.M., Kroetz, D.L., Kwok, P.-.Y., 2013. OATP1B1-related drug–drug and drug–gene interactions as potential risk factors for cerivastatin-induced rhabdomyolysis. Pharmacogenet. Genomics 23, 355–364. https://doi.org/10.1097/FPC.0b013e3283620c3b.

Tatosian, D.A., Yee, K.L., Zhang, Z., Mostoller, K., Paul, E., Sutradhar, S., Larson, P., Chhibber, A., Wen, J., Wang, Y.J., Lassman, M., Latham, A.H., Pang, J., Crumley, T., Gillespie, A., Marricco, N.C., Marenco, T., Murphy, M., Lasseter, K.C., Marbury, T.C., Tweedie, D., Chu, X., Evers, R., Stoch, S.A., 2021. A microdose cocktail to evaluate drug interactions in patients with renal impairment. Clin. Pharmacol. Ther. 109, 403–415. https://doi.org/10.1002/cpt.1998.

Taylor-Wells, J., Meredith, D., 2014. The signature sequence region of the human drug transporter organic anion transporting polypeptide 1B1 is important for protein surface expression. J. Drug Deliv. 2014, 1–10. https://doi.org/10.1155/2014/129849.

Tikkanen, A., Pierrot, E., Deng, F., Sánchez, V.B., Hagström, M., Koenderink, J.B., Kidron, H., 2020. Food additives as inhibitors of intestinal drug transporter OATP2B1. Mol. Pharm. 17, 3748–3758. https://doi.org/10.1021/acs.molpharmaceut.0c00507.

Tirona, R.G., Leake, B.F., Merino, G., Kim, R.B., 2001. Polymorphisms in OATP-C: identification of multiple allelic variants associated with altered transport activity among European- and African-Americans. J. Biol. Chem. 276, 35669–35675. https://doi.org/10.1074/jbc.M103792200.

Tirona, R.G., Leake, B.F., Wolkoff, A.W., Kim, R.B., 2003. Human Organic anion transporting polypeptide-C (SLC21A6) is a major determinant of rifampin-mediated pregnane X receptor activation. J. Pharmacol. Exp. Ther. 304, 223–228. https://doi.org/10.1124/jpet.102.043026.

Tzeng, T.-.B., Schneck, D.W., Birmingham, B.K., Mitchell, P.D., Zhang, H., Martin, P.D., Kung, L.P., 2008. Population pharmacokinetics of rosuvastatin: implications of renal impairment, race, and dyslipidaemia. Curr. Med. Res. Opin. 24, 2575–2585. https://doi.org/10.1185/03007990802312807.

Weaver, Y.M., Hagenbuch, B., 2010. Several conserved positively charged amino acids in OATP1B1 are involved in binding or translocation of different substrates. J. Membr. Biol. 236, 279–290. https://doi.org/10.1007/s00232-010-9300-3.

Weng, T.C., Yang, YH.K., Lin, S.J., Tai, S.H., 2010. A systematic review and meta-analysis on the therapeutic equivalence of statins. J. Clin. Pharm. Ther. 35, 139–151. https://doi.org/10.1111/j.1365-2710.2009.01085.x.

Wu, H.F., Hristeva, N., Chang, J., Liang, X., Li, R., Frassetto, L., Benet, L.Z., 2017. Rosuvastatin Pharmacokinetics in Asian and White Subjects Wild Type for Both OATP1B1 and BCRP under control and inhibited conditions. J. Pharm. Sci. 106, 2751–2757. https://doi.org/10.1016/j.xphs.2017.03.027.

Zhang, Y., Panfen, E., Fancher, M., Sinz, M., Marathe, P., Shen, H., 2019. Dissecting the contribution of OATP1B1 to hepatic uptake of statins using the OATP1B1 Selective inhibitor estropipate. Mol. Pharm. 16, 2342–2353. https://doi.org/10.1021/acs.molpharmaceut.8b01226.